7th Int. Symp. "Nanostructures: Physics and Technology"
St Petersburg, Russia, June 14–18, 1999

Influence of initial MBE growth stage on properties of hexagonal InN/Al_2O_3 films

V. V. Mamutin, V. A. Vekshin, V. Yu. Davydov, V. V. Ratnikov,
V. V. Emtsev, A. N. Smirnov, S. V. Ivanov and P. S. Kop'ev
Ioffe Physico-Technical Institute, St Petersburg, Russia

Abstract. The InGaN alloys have acquired a lot of interest for using in the active region of light emitting and lasers diodes, as the band gap of this materials can be varied over nearly the whole visible spectral range, when changing In content from 0 to pure InN [1]. However, due to the low dissociation temperature of InN (about 630°C [2]) and the nitrogen equilibrium vapor pressure with a growth temperature (T_s) [3], good quality InN epilayers are still not easily attainable. Taking account of the large lattice mismatch between InN and sapphire, it is also expected that a strain-induced enhanced N re-evaporation at the initial InN monolayer growth [4] would require a 100–150°C decrease of T_s to avoid a liquid In droplet formation followed by a columnar structure growth. As a result, there are only few papers, to our knowledge, on epitaxial InN properties [5–7], and no reports on hexagonal InN films MBE growth.

1 Experimental

InN epilayers were grown on (0001) sapphire substrates by MBE. The MBE chamber (home made EP-1203 setup) with ultimate background pressure $\sim 10^{-10}$ Torr was equipped with a turbomolecular pump with an effective pumping rate of $\sim$ 350 l/s). Metallic In was supplied by a standard effusion cell at a temperature varied within a 750–850°C range in a series of experiments. ASTEX ECR plasma source was used for supplying activated nitrogen with flow rate of about 1–5 sccm, allowing the growth rates of 0.02–0.20 μ/h. The substrates were coated with Ti at back side and mounted on In-free Mo holders. Before loading, sapphire substrates were rinsed in acetone only and then thermally cleaned and nitridated at $\sim$ 1100–1200°C for 30 min, demonstrating finally streaky reflection high energy electron diffraction (RHEED) pattern. T_s for main InN layer growth was varied from 350 to 550°C. Its calibration procedure involved adjusting to several metal melting points, using IR pyrometer and a temperature versus heater power dependence, and provided an $\sim$ 10°C accuracy. Surface structure of the InN epilayers during growth was also monitored by RHEED. The film thickness was in between 0.1 and 0.7 μm.

Three different growth initiation regimes were used. In the first one (I), the growth of main InN epilayer started immediately after high temperature substrate annealing, when T_s was reduced to the working value. In the second regime (II), a $\sim$ 15 nm thick low temperature InN buffer layer was first grown at $\sim$ 300°C, followed by rising T_s to the value of the main InN growth. The third initiation regime (III) differed from the second one by high temperature ($\sim$ 800–900°C) annealing of the low temperature InN buffer before growth of the main InN layer.

Structural and morphological characterization of InN/Al_2O_3 epilayers was performed by high resolution triple-crystal X-ray diffraction (TC XRD), Raman scattering, and scanning electron microscopy (SEM). The symmetrical and asymmetrical Bragg geometry and CuK_α radiation were used for measurements of XRD rocking curves in the vicinity of 0002, 0004 and $11\bar{2}4$ reflections. The full width at half maximum for and $(\Theta - 2\Theta)$ -

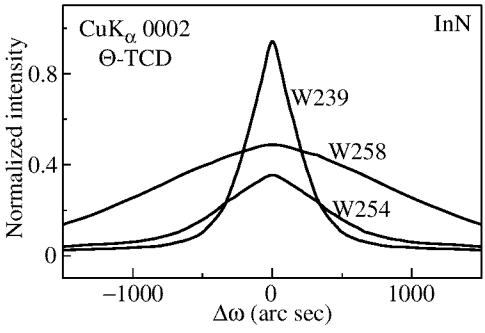

Fig. 1. Θ-TCD curves for MBE InN layers.

scans (ω_Θ and $\omega_{\Theta-2\Theta}$ respectively) was analysed. The curvature radius measurements were employed for a stress calculation in the layers. The Raman spectra of InN layers were measured at room and cryogenic temperatures (at 6 K). Ar^+ ($\lambda_0 = 514$, 488 and 476 nm) and Kr^+ ($\lambda_0 = 647$ and 674 nm) lasers were used for excitation. A carrier concentration was determined by Hall-effect measurements.

2 Results and discussion

MBE growth of complete InN layer in the regime I turns out to be possible at $T_S \sim 350°C$. However, RHEED patterns for the epilayer (W258) corresponds to a polycrystalline or textural 3D-growth (spots, rings and strokes on the rings) from the very beginning of growth. SEM image shows a rough surface and columnar structure at the cleavage. In contrast, regimes II (W254) and III (W239) allow the main InN layer to be grown at maximal possible $T_S \sim 470°C$, when the In/N flux ratio is close to 1:1 and In droplets do not occur. This temperature agrees well with a lower boundary of theoretically estimated region of droplet free InN growth [3]. RHEED for both InN layers demonstrates streaky patterns corresponding to a 2D-growth. Their SEM images show flat surface without columnar structure. However, the InN layer grown in the regime II contains cavities at the InN/Al_2O_3 interface, which are completely recovered after ~ 0.01 μm growth, whereas only the layer III (W239) has a flawless interface with sapphire.

XRD study reveals only hexagonal InN phase for all the samples. The InN layers has a Gaussian shape of rocking curves which is characteristic for III-N's (see Fig. 1). The analysis has shown an asymmetry of diffraction spot elongated parallel to the surface of samples W239 and W254. According to [8] this effect is caused by a small block size anysotropy and specific defect structure of blocks (vertical screw and edge dislocations). The values of lateral block size τ_x and vertical screw dislocation density ρ^{vsd} are given in the Table. For the W258 sample, XRD scattering is almost anysotropical and is mainly determined by small tilted blocks. The stresses σ_a in the layers are biaxial compressive ones (see the Table). The samples W254 and W258 are fully relaxed as a result of layer fragmentation to small blocks.

The analysis of Raman data suggests that the samples under study are epitaxial structures of hexagonal symmetry with the optical axis normal to the substrate plane. No traces of cubic phase have been detected. According to the group-theory analysis, six optical modes, i.e. $A_1(TO) + A_1(LO) + E_1(TO) + E_1(LO) + E_2^1 + E_2^2$, can be observed for the first-order Raman scattering in a hexagonal InN. Some of the spectra taken from InN samples at 300 K, $\lambda_0 = 488$ nm (2.54 eV) are presented in Fig. 2(a). These spectra have been obtained in the scattering configurations allowing the nonpolar E_2^1 and E_2^2 modes for

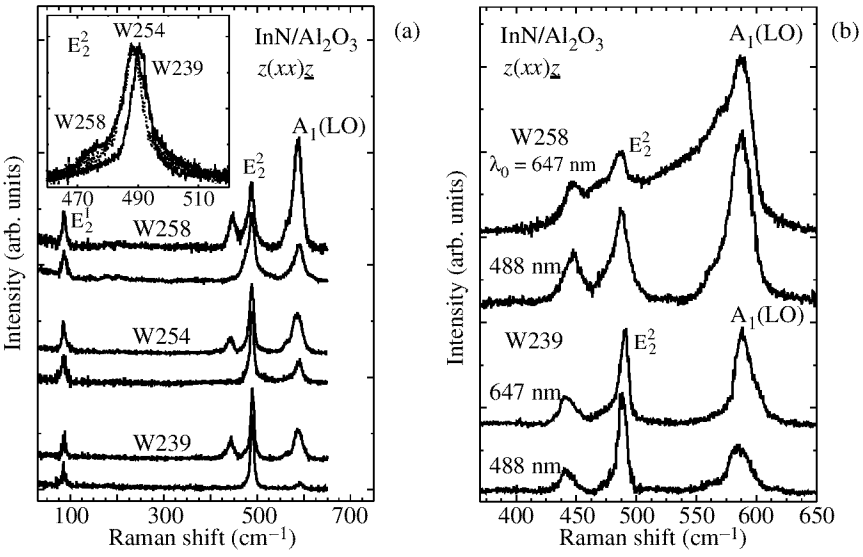

Fig. 2. (a) Raman spectra for InN samples grown in different conditions. (b) Raman spectra obtained with different energies of excitation.

Table 1. The characterization data obtained for InN samples by different techniques

Regime (sample)	σ_a GPa	τ_x 10^{-4} cm	ρ^{vsd} 10^9 cm^{-2}	ω_Θ (0002) arc sec	$\omega_{\Theta-2\Theta}$ (0002) arc sec	FWHM cm^{-1}	n $10^{20}\mu$ cm^{-3}	cm^2/Vs
I-W258	~ 0	< 0.1	$\gg 1$	2140	174	9.6	4	93
II-W254	~ 0	~ 0	1.0	777	80	7.1	2	160
III-W239	-1.23	> 0.5	0.2	350	55	6.2	1	600

both polarizations. However, the longitudinal component of the polar A_1(LO) mode is allowed only in $z(xx)\underline{z}$ polarization. Here the z direction is parallel to the optical c axis. It is clearly seen that the polarized Raman spectra for W239 sample show an excellent agreement with the selection rules, while for W254 and W258 samples selection rules are broken. The inset in Fig. 2(a) shows high-resolution Raman spectra recorded in the region of the E_2 symmetry phonon. The results of fitting of the E_2 line to the Lorentz function (FWHM) are also presented in Table. The large FWHM of E_2 for W258 sample points to the presence of a considerable amount of structural defects in this sample. Using different energies of excitations, we tested different depth of InN layers. Some of the results are presented in Fig. 2(b). It is clearly seen that the Raman spectra of W239 sample are nearly identical for both energies of excitation. This is the evidence of structural uniformity of this sample through the whole thickness. However there is a strong additional band in the Raman spectrum of W258 sample for $\lambda_0 = 647$ nm (1.92 eV) excitation. This band is due to defect induced Raman scattering and shows that the defects are placed near the interface of W258 InN film.

It is known that the E_2 mode is extremely sensitive to the strain in III-N's compounds. For example in GaN layers, the shift of this line by 2.7 cm^{-1} corresponds to the in-plane biaxial stress equal to 1 GPa [9]. The shift of the E_2 line toward higher frequencies

with respect to its position for the strain-free sample W254 ($\Delta = 2.1\,\mathrm{cm}^{-1}$) indicates the compressive in-plane biaxial stress in the sample W239 (see insert in Fig. 2(a)). According to the Raman data, the residual strain in the W258 sample relaxes totally. Thus, the set of all Raman data for investigated InN samples agrees well with the XRD data.

The results of Hall measurements, summarized in the Table, confirm these results, demonstrating the lower electron concentration and higher mobility for the W239 sample, grown with the initiation regime III. As a possible reason of these effects, we suggest that high temperature annealing of the buffer layer results in the formation of an interface nucleation layer of gradual composition (most probably, $Al_xIn_{1-x}N$), which provides a lower lattice mismatch for the main InN layer, preventing the In droplet formation at the InN/AlInN/Al_2O_3 interface at high temperatures. The detailed study of this interface will be published elsewhere. These results can be used for a study of self-organization phenomena in MBE of InN/GaN nanostructures.

3 Conclusion

In summary, we have studied the influence of initial growth stages on the quality of InN MBE layers using SEM, XRD, Raman scattering, Hall-effect measurements. It has been shown that the high temperature annealing of low temperature grown InN buffer layer, followed by the main InN layer growth at maximal T_s permitting In/N = 1:1 growth condition, provides the high quality strained films with featureless InN/sapphire interface.

This work is partly supported by RFBR Grants (No 99-02-17103 and No 99-02-18318), and the Program of the Ministry of Sciences of RF "Physics of Solid State Nanostructures".

References

[1] S. Strite and H. Morkoc, *J. Vac. Sci. Technol.* **B10**, 1237 (1992).
[2] T. Bottcher, S. Einfeldt, V. Kirchner, S. Figge, H. Heinke and D. Hommel, *Appl. Phys. Lett.* **73**, 3232 (1998).
[3] S. Y. Karpov, Y. N. Makarov and M. S. Ramm, *Internet J. Nitride Sem.* Res. 2, Art. 45.
[4] S. V. Ivanov, *et al.*, *Semicond. Sci. Technol.* **8**, 347 (1993).
[5] H. J. Kwon, Y. H. Lee, O. Miki, H. Yamano and A. Yoshida, *Appl. Phys. Lett.* **69**, 937 (1996).
[6] K. Osamura, S. Naka and Y. Murakami, *J. Appl. Phys.* **46**, 3432 (1975).
[7] M. C. Lee, *et al. Appl. Phys. Lett.* **73**, 2606 (1998).
[8] R. N. Kutt, V. V. Ratnikov, G. N. Mosina and M. P. Scheglov, *Solid St. Phys.* **41**, 28 (1999).
[9] V. Yu. Davydov, N. S. Averkiev, I. N. Goncharuk, *et al J. Appl. Phys.* **82**, 5097 (1997).